

OXALIC ACID PRODUCTION IN THE COASTAL MARINE ATMOSPHERE

Kathleen K. Crahan*, Dean Hegg, David S. Covert and H. Jonsson
University of Washington, Seattle, WA

Oxalic acid, a C₂ dicarboxylic acid, is the most abundant dicarboxylic acid in aerosols in both urban and remote atmospheres, and often a significant contributor to the overall organic mass content of aerosols. Although oxalic acid is known to be a byproduct of automobile exhaust, its omnipresence in remote atmospheres, coupled with its limited estimated lifetime of six to twelve days, suggest a mechanism for its formation from natural precursors as well. Recently two pathways for oxalic acid formation in cloud water have been proposed by Warnick (2003; see Figure 1).

CARMA (Cloud-Aerosol Research in the Marine Atmosphere I) took place off the California coast in August and September of 2002. The CIRPAS (Center for Interdisciplinary Remotely-Piloted Aircraft Studies) Twin Otter aircraft was the primary research platform used for data collection and was equipped with a number of instruments to quantify meteorological conditions, cloud properties, gas phase concentrations and aerosol physical and chemical properties. Included in these instruments were the modified Mohen slotted cloud water collector as described by Hegg *et al.* (1986) and an aerosol filter sampler. The chemical speciation of the collected aerosols was determined in the laboratory as described by Gao *et al.* (2003). Three times the standard deviation of the blanks was used as the detection limit for the aerosols, and was found to be at 24 ppb for sulfate and 4.0 ppb for oxalate. The error associated with these two ions was 4% and 6%, respectively. Additionally, aerosol size and mass distributions were determined during the flights with the external optical probes PCASP-100x and FSSP-100 (PMS/DMT Inc., Boulder, Co), and with the Micro Orifice Uniform Deposit Impactor (MOUDI). The MOUDI is a five stage impactor with aerosol diameter cut-offs at 2.5 μm , 1.4 μm , 0.77 μm , 0.44 μm and

0.26 μm and is equipped with a backup filter to collect the remaining aerosols.

The first piece of evidence supporting the proposed cloud-water formation mechanism is the similarity in the size distribution of the sulfate-containing aerosols and oxalate-containing aerosols in the below-cloud aerosol samples taken by the MOUDI. Figure 2 and Figure 3 illustrate the peaks in both nss sulfate and oxalate size distributions are found between the aerosol diameter of 0.44 μm and 0.26 μm , which is reflected in the smaller mode revealed by the simultaneous PCASP measurements. This is likely to be the droplet mode, formed by evaporating cloud droplets (Kerminen and Wexler, 1995; Blando and Turpin, 2000). Sufficiently long sample times for significant oxalate mass deposition on the MOUDI substrates occurred on only two days.

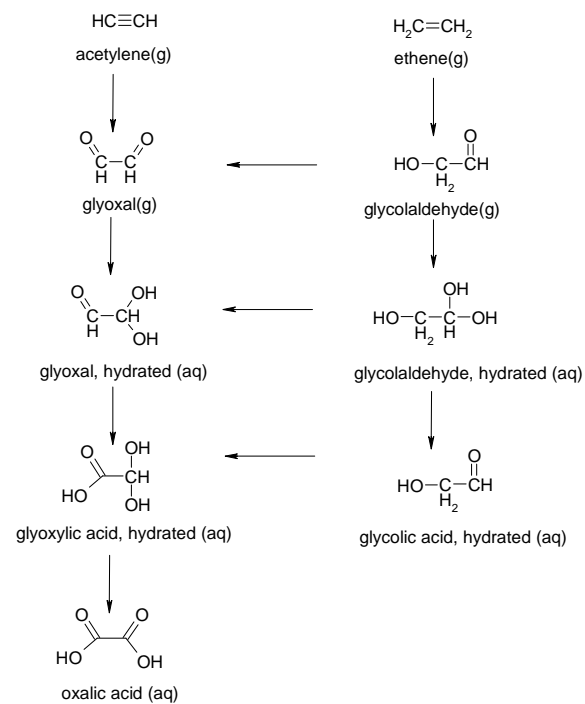


Figure 1: The proposed reaction pathway for the formation of oxalic acid in cloud water.

*Corresponding Author: Kathleen Crahan, Dept. of Atmospheric Science, Box 351640, University of Washington, Seattle, Washington 98195-1640. Email: katie@atmos.washington.edu

Filter	Date	Altitude (m)	NSS-Sulfate ($\mu\text{g m}^{-3}$)	Oxalate ($\mu\text{g m}^{-3}$)
TO-10	24-Aug	BC: 180	1.12	0.089
8/24 3	24-Aug	IC: 430	3.31	0.164
8/24 1	24-Aug	IC: 522	2.19	0.222
8/24 2	24-Aug	IC: 530	1.13	0.095
TO-15	26-Aug	BC: 180	1.05	0.104
8/26 1*	26-Aug	IC: 180		
TO-22	28-Aug	BC: 240	1.30	0.143
8/28 1*	28-Aug	IC: 365	1.81	0.161
8/28 2	28-Aug	IC: 406	2.11	0.293
TO-24	29-Aug	BC: 180	0.33	0.027
8/29 2**	29-Aug	IC: 402	0.67	0.110
8/29 1**	29-Aug	IC: 407	0.87	0.069
TO-28	30-Aug	BC: 90	0.547	0.028
8/30 2*	30-Aug	IC: 286	0.97	0.132
8/30 1*	30-Aug	IC: 288	1.161	0.125
TO-34	31-Aug	BC: 180	0.91	0.088
8/31 2	31-Aug	IC: 241	6.07	0.401
8/31 1	31-Aug	IC: 408	2.05	0.251
TO-42	3-Sep	BC: 200		0.107
9/3 2	3-Sep	IC: 287	3.11	0.517
Average in-cloud production			1.66	0.108

Table 1: A comparison of the in-cloud concentrations of nss sulfate and oxalate to concentrations observed below-cloud. BC indicates aerosols collected below-cloud, while IC indicates aerosols collected in cloud drops and droplets.

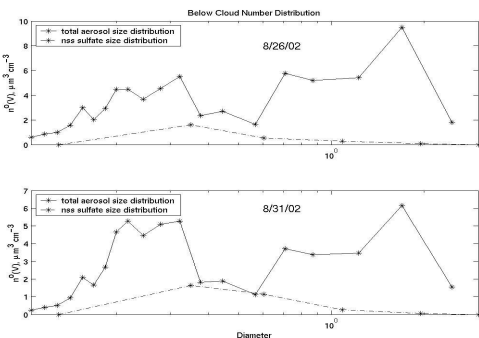


Figure 2: Comparison of total aerosol size distribution from PCASP and simultaneous nss sulfate aerosol size distributions derived from MOUDI data.

The in-cloud and below-cloud total concentrations of nss sulfate and oxalate were determined directly after the field campaign, and the results are reported in Table 1. The air equivalent concentration was found by multiplying the average cloud liquid water content with the cloud water chemical concentration as determined from IC analysis. On average, over twice as much sulfate was found in-cloud than below-cloud, which we attribute to in-cloud sulfate production. Similarly, there is approximately three times as much oxalate found in cloud as there is below cloud, suggesting an in-cloud production pathway for oxalate as well.

The IC also has the capacity to detect glyoxylic acid and glycolic acid, proposed oxalic acid.

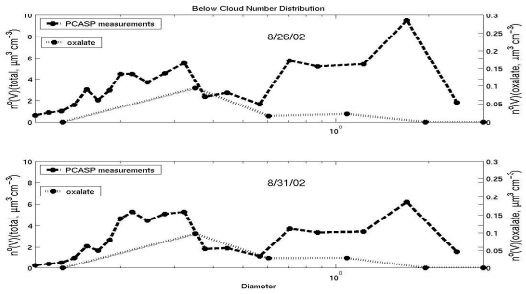


Figure 3: Comparison of total aerosol size distribution from PCASP and simultaneous oxalate aerosol size distributions derived from MOUDI data.precursors.

Although such analyses were not initially carried out, the IC data collected for the cloud water samples were later reviewed to address this question (due to the time elapsed between the initial analysis of the cloud water and the subsequent search for oxalic acid production precursors, reanalysis of the cloud water using the IC was infeasible because of the breakdown of organic acids). The glycolic peak is commonly subsumed in the formate peak for the analytical conditions (e.g. eluent strength, flow rate, etc.) at which the cloud water was analyzed. The glyoxylic acid peak may also be engulfed within a strong chloride peak. Nevertheless, when the in-cloud chloride concentration was less than $55 \mu\text{g cl}^{-1}$, a peak, attributable to glyoxylate, was detected on the leading shoulder of the chloride peak in a total of five cloud water samples. A similar peak was not detected in the aerosol samples collected below cloud, as would be expected if correspondingly low concentrations of glyoxylic acid were in the aerosol. At the time of reanalysis, a set of standards were run through the IC to ascertain the elution time of glyoxylate and the concentrations at which glyoxylic acid was found in the cloud water samples.

The time between the initial analysis of the cloud water and the subsequent identification of the glyoxylate peak, coupled with the one-dimensionality of the chemical analysis techniques leads to only a tentative identification of the glyoxylic peak. Over time, the IC is susceptible to instrumental drift due to subtle variations in the mobile phase and stationary phase volume, and thus the peak retention time is not an accurate way to identify an analyte. However, the IC selectivity factor can also be used to support the existence of the glyoxylate

peak. The selectivity factor is a ratio of k for two different analytes for the same analysis, where k is the ratio of moles of the analyte in the mobile phase of the IC analysis to the moles in the stationary phase, and can be estimated by subtracting the dead time of the IC run from the retention time and then dividing the difference by the dead time. This leads to $\alpha = (t_{r,\text{Cl}} - t_{0,\text{Cl}})/(t_{r,g} - t_{0,g})$, where α is the selectivity factor, t_r is the retention time, t_0 is the dead time, and the subscripts Cl and g refer to chloride and glyoxylic acid, respectively. This provides support for the glyoxylic peak identification, as it is independent of the volume of the stationary phase and mobile phase, and thus not susceptible to instrumental drift. The two standards that contained both glyoxylic acid and chloride had a mean selectivity factor of 1.22 ± 0.01 (standard deviation), while the five cloud water samples had a mean of 1.25 ± 0.03 .

The concentration of the glyoxylic acid found in cloud water was calculated using regression analysis and had an estimated error of $0.07 \mu\text{g cl}^{-1}$. The results of the glyoxylic acid IC analysis with corresponding oxalate peaks are seen in Figure 4. Note that the anomalously high oxalate peak observed on the 23rd of August is reflected by high concentrations of malonic, succinic and glutaric acids. The presence of levoglucosan in the sample, not found in any of the other samples shown in Figure 4, suggest that the additional source of dicarboxylic acids present may due to biomass burning, for this particular case.

While the oxalic acid contributes only a small portion to the total mass of the aerosol population (less than 3% on average during CARMA I), it may contribute a significant amount

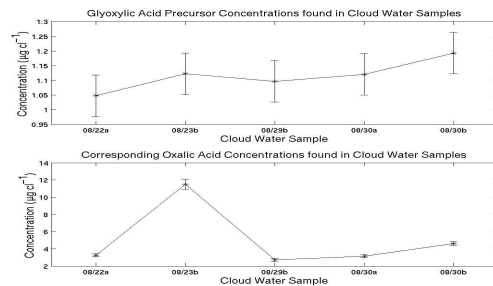


Figure 4: Glyoxylic acid and oxalic acid concentrations and error bars identified in cloud water samples using ion chromatography detection techniques.

to the smaller sized aerosol population, increasing the number of cloud condensation to the smaller sized aerosol population, increasing the number of cloud condensation nuclei

available for activation, thus possibly impacting cloud albedo and cloud lifetime. Based upon the data gathered by the CARMA I field campaign, further study of the aqueous production pathway of oxalic acid and its implications is warranted.

References:

Blando, J. D., and B. J. Turpin, 2000: Secondary organic aerosol formation in cloud and fog droplets: a literature evaluation of plausibility. *Atmos. Environ.*, **34**, 1623-1632.

Gao, S., D. A. Hegg, D. S. Covert and H. Jonsson, 2003: Aerosol chemistry, and light-scattering and hygroscopicity budgets during outflow from East Asia. *J. Atmos. Chem.*, **46**, 55-88.

Hegg, D. A. and P. V. Hobbs, 1986: Sulfate and nitrate chemistry in marine cumuliform clouds. *Atmos. Environ.*, **20**, 901-909.

Kerminen, V. M. and A. S. Wexler, 1995: Growth laws for atmospheric aerosol particles: an examination of the bimodality of the accumulation mode. *Atmos. Environ.*, **29**, 3263-3275.

Warnick, P., 2003: In-cloud chemistry opens pathway to the formation of oxalic acid in the marine atmosphere. *Atmos. Environ.*, **37**, 2423-2427.